Publication II

Olli Himanen, Tero Hottinen, "*Characterization of membrane electrode assembly with hydrogen-hydrogen cell and ac-impedance spectroscopy Part II. Modeling*", Electrochimica Acta 52, pp. 581-588, 2006

Available online at www.sciencedirect.com
ScienceDirect
Electrochimica Acta 52 (2006) 581–588
ELECTROCHIMICA Acta
www.elsevier.com/locate/electacta

Characterization of membrane–electrode assembly with hydrogen–hydrogen cell and ac-impedance spectroscopy Part II. Modeling

Olli Himanen *, Tero Hottinen

Helsinki University of Technology, Laboratory of Advanced Energy Systems, P.O. Box 2200, 02015 HUT, Finland

Received 18 January 2006; received in revised form 26 April 2006; accepted 16 May 2006
Available online 7 July 2006

Abstract

A two-dimensional, one-phase model for hydrogen and water vapor transport inside a hydrogen–hydrogen cell is presented. The model was used to analyze the results of water transport measurements. As a result, the concentration dependence of the diffusion coefficient of water in membrane of Gore™ Primea® Series 58 MEA was achieved. Temperature differences inside a hydrogen–hydrogen cell were studied with modeling approach and it was found that the cell can be treated as an isothermal system.

Keywords: PEMFC; Hydrogen–hydrogen cell; Water transport; Non-isothermal; Membrane conductivity

1. Introduction

Perfluorosulfonic acid polymer membranes used in polymer electrolyte membrane fuel cells need water to conduct protons properly. However, excess water may result in electrode flooding causing mass transport limitations. Thus, it is important to find a balance between these two opposite factors to maximize the cell performance. In order to be able to develop and choose materials for fuel cells, their water transport properties must be known.

The use of a symmetrical H_2–H_2 cell is one possible method to study water transport properties of polymer membrane. H_2–H_2 cell enables the measurement of water transport through the membrane under the similar conditions as PEMFC is operating (same components, same assembly pressure, same transport mechanism). With H_2–H_2 cell it is possible to directly measure the diffusive water flux through the membrane, whereas with ex situ measurements (NMR) the diffusive water flux is not measured, and the diffusion coefficient is calculated from other measurement parameters. The conditions of ex situ measurements are different than in operating fuel cell. However, the concentration of water in the membrane is not uniform when H_2–H_2 cell technique is used to study water transport properties and only average values for diffusion coefficient can be achieved directly from such measurement results. Thus, modeling work is needed in order to achieve more accurate parameter values.

In this work, a theoretical model for water transport inside the cell components is presented and used to analyze results of net water flux measurements conducted with a H_2–H_2 cell. The model includes one-phase transport of hydrogen and water vapor in porous cell components and diffusive water transport through the membrane. The measurement results given in [1] are used as material parameters and boundary conditions. Measurements were made using Gore™ Primea® Series 58 MEA. As a result of the modeling work, the concentration dependence of the diffusion coefficient of water in the membrane is obtained.

Most of the transport and electrochemical processes are temperature dependent. Therefore, temperature distribution inside a hydrogen–hydrogen cell was also modeled and it was noticed that the cell can be treated as an isothermal system. Heat was assumed to be transferred by conduction and convection, and produced by reaction entropy, activation losses, water phase change, and ohmic heating both in bulk components and at interfaces.

* Corresponding author.
E-mail address: olli.himanen@tkk.fi (O. Himanen).

0013-4686/$ – see front matter © 2006 Elsevier Ltd. All rights reserved.
doi:10.1016/j.electacta.2006.05.037

2. 2D-model for water transport inside the cell

The calculation of the membrane transport properties requires that the water concentration profile at the membrane surface is known. Using the measurement technique described in [1], the concentrations of water at the inlet and outlet can be measured, but the concentration profile of water inside the cell and especially along the membrane surface is unknown. A 2D-model for the mass transport was developed to gain insight into the water distribution inside the H_2–H_2 cell used in [1]. The model was also used to find out the concentration dependence of the diffusion coefficient of water in the membrane.

The model is isothermal and includes transport phenomena of hydrogen and water vapor inside the flow field nets, gas diffusion backings, and electrodes, and also water transport inside the membrane. Mass transport inside the flow field nets, gas diffusion backings, and electrodes are modeled using Darcy's equation for convective transport, Fick's equation for diffusive transport, and the continuity equation. Liquid water transport and phase change phenomena are not taken into account in this model, and therefore the modeling is limited to one-phase conditions. Because of this limitation only those measurement results in [1], which were achieved under one-phase conditions were analyzed with this model. The dew point-temperature of water vapor was at least 2 °C lower than the temperature of the cell components. Therefore all water should be in vapor form inside the cell. The measurements, in which the dew-point temperature of the water vapor was higher than the cell temperature, were not used in the determination of diffusion coefficient of water.

The model geometry is illustrated in Fig. 1. Because the H_2–H_2 cell used in the measurements [1] is cylindrically symmetric, only half of the cross-section of the cell has to be modeled. Left boundary of the model geometry in Fig. 1 is the centre line of the cell and is treated with symmetry boundary conditions.

Hydrogen–water vapor mixture is fed into the cell through the inlet boundaries. The gas mixture flows inside the flow field nets, gas diffusion backings and electrodes towards the outlet boundaries. When the water vapor is in contact with the membrane surface, the membrane absorbs a certain amount of water. The relation between the concentration of water inside the membrane and in the gas phase is called a water uptake isotherm. The concentration gradient of water across the membrane causes water to diffuse through the membrane. The water flux through the membrane is modeled with the Fick diffusion equation assuming that the diffusion coefficient of water in the membrane is concentration dependent. The dependence of the diffusion coefficient was varied until the concentrations of water vapor in the outlet gas streams matched the measurement results. The equations used in the model are described in the following subchapters.

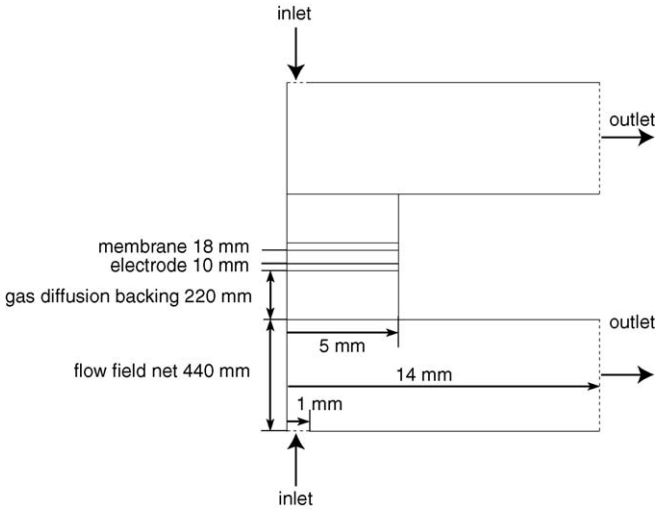

Fig. 1. Modeled geometry. Gas inlet and outlet boundaries are marked with dashed lines.

2.1. Flow field nets, gas diffusion backings and electrodes

The convective velocity of hydrogen–water vapor mixture is assumed to be the same as the convective velocity of hydrogen because the amount of water in the mixture is relatively small. The validity of this assumption will be discussed in the results chapter. The convective mass flux of hydrogen is calculated using the Darcy equation and the continuity equation

$$\nabla \cdot (\rho \vec{v}) = \nabla \cdot \left(-\frac{pM}{RT} \frac{\kappa}{\eta} \nabla p \right) = 0, \tag{1}$$

where ρ is the density of hydrogen, $\vec{v}$ the convective velocity of hydrogen in the laboratory coordinate system, p the pressure of hydrogen, M the molar weight of hydrogen, R the molar gas constant, T the absolute temperature, κ the hydraulic permeability of the media, and η the dynamic viscosity of hydrogen. All parameters are calculated at 35 °C and 100 kPa.

The convective flux at the inlet is assumed to be fully developed Poiseuille flow, and can be calculated from the known total volumetric flow of hydrogen. Thus, the boundary condition for the velocity profile at the inlet is

$$v(r) = 2.65 \times 10^6\,\mathrm{m^{-1}\,s^{-1}}(1 \times 10^{-6}\,\mathrm{m^2} - r^2), \tag{2}$$

where r is the distance from the center of the inlet channel, i.e. from the left boundary of the modeled geometry.

At the outlet boundaries the pressure is fixed to the ambient pressure, 100 kPa. Due to the cell geometry, symmetry condition is applied onto the left boundary, and thus all fluxes through that boundary are set to zero. The membrane is assumed to be gas impermeable, and therefore convective velocities through the boundaries between the membrane and electrodes are set to zero. Hence, the only flux through the membrane–electrode boundary is the diffusive water flux. The remaining boundaries are bounded by current collectors, cell body or gaskets, and therefore the fluxes through these boundaries are set to zero.

Molar flux of water vapor is calculated as a sum of convective and diffusive fluxes

$$\vec{J}_{H_2O} = \vec{v} c_{H_2O} - D_{H_2,H_2O} \varepsilon^{1.5} \nabla c_{H_2O}, \tag{3}$$

where $\vec{J}_{H_2O}$ is the molar flux of water, c_{H_2O} is the concentration of water vapor, D_{H_2,H_2O} is the diffusion coefficient between

hydrogen and water vapor and ε is the porosity of media. The Bruggemann correlation is used to take into account the effects of porosity and tortuosity on the diffusion coefficient. The diffusion coefficient between hydrogen and water vapor is calculated using the Fuller correlation [2].

Because there are no water sources or sinks in the flow field nets, gas diffusion backings and electrodes, the divergence of the water flux is zero

$$\nabla.(\vec{v}c_{H_2O} - D_{H_2,H_2O}\varepsilon^{1.5}\nabla c_{H_2O}) = 0 \quad (4)$$

Boundary conditions are the known concentration of water vapor at the inlet boundaries and an assumption that the diffusion flux is zero at the outlet boundary. This boundary condition means that the concentration of water vapor at the outlet boundary is not fixed and is dependent on the water transport through the membrane. This allows the fitting of the model into measurement results.

2.2. The membrane

The only mechanism for water transport through the membrane is assumed to be Fick diffusion. Water transport measurements were made in open-circuit mode and therefore current through the membrane and water transport by electro-osmotic drag are zero. Water transport by hydraulic permeation is also nonexistent, because there is no pressure gradient over the membrane. Water flux in the membrane is calculated with the Fick diffusion equation

$$\vec{J}_{H_2O} = -D_{H_2O,membrane}\nabla c_{H_2O,membrane}, \quad (5)$$

where $D_{H_2O,membrane}$ is the Fick diffusion coefficient of water in the membrane, and $c_{H_2O,membrane}$ is the concentration of water in the membrane. There are no water sources or sinks in the membrane, and thus the divergence of the water flux is zero

$$\nabla \cdot (-D_{H_2O,membrane}\nabla c_{H_2O,membrane}) = 0. \quad (6)$$

The boundary condition at the membrane–electrode interface is based on the water uptake of the membrane

$$c_{H_2O,membrane} = \frac{WU(c_{H_2O})\rho_{membrane}}{M_{H_2O}}, \quad (7)$$

where $\rho_{membrane}$ is the density of the dry membrane and $WU(c_{H_2O})$ is the water uptake of the membrane calculated from the concentration of water vapor at the electrode–membrane boundary. It must be noted that the water uptake of membrane without the electrodes was not measured and was assumed to be the same as the water uptake of the whole MEA [1]. The water uptake was measured to be [1]

$$WU(c_{H_2O}) = 0.0012 - 0.00043c_{H_2O} + 0.014c_{H_2O}. \quad (8)$$

The dependence of the diffusion coefficient of water on the concentration of water was assumed to obey an exponential relation

$$D_{H_2O,membrane} = D_0\left(1 - \exp\left(\frac{c_{H_2O,membrane}}{c_{H_2O,sat}}\right)\right), \quad (9)$$

where D_0 is the parameter of the model, $c_{H_2O,membrane}$ is the concentration of water in the membrane and $c_{H_2O,sat}$ is the concentration of water in the membrane stabilized with saturated water vapor. The value of $c_{H_2O,sat}$ can be calculated using Eqs. (7) and (8) and it is 7521 mol m^{-3}. The dependence given in Eq. (9) was developed because it has only one free parameter to be fitted and it gives qualitatively similar behavior as that measured for water self-diffusion coefficient in Nafion® 117 by Zawodzinski et al. [3].

2.3. Computational methods and parameter values

The objective of the modeling work was to solve the water distribution inside the cell and to find the dependence of the water diffusion coefficient in the membrane on water concentration. The equation system described in Sections 2.1 and 2.2 was solved with a commercial finite element method solver COMSOL Multiphysics™ running on a computer equipped with AMD64 3500+ processor, 4 GB RAM, and SUSE Linux 9.1 AMD64 operating system.

Parameter values used in the modeling are given in Table 1. The porosity of the compressed gas diffusion backing is calculated from the porosity of uncompressed GDB given in [4], assuming that the porosity is directly related to the thickness. The porosity and thickness of uncopressed SGL-10BA GDB are, 0.877 and 380 μm. The thickness of compressed GDB was 220 μm and therefore its porosity was estimated to be 0.51.

Table 1
Parameter values used in the water transport model

Parameter	Value	Reference
Porosity of gas diffusion backing (ε_{GDB})	0.51	Calculated from [4]
Porosity of flow field net (ε_{net})	0.427	Manufacturer of the net
Porosity of electrode ($\varepsilon_{electrode}$)	0.4	Used in [5]
Permeability of flow field net (κ_{net})	4.2×10^{-10} m^2	[1]
Permeability of gas diffusion backing (κ_{GDB})	1.2×10^{-11} m^2	[1]
Permeability of electrode ($\kappa_{electrode}$)	1.26×10^{-13} m^2	[1]
Diffusion coefficient of H_2 in H_2O (D_{H_2,H_2O})	9.43×10^{-5} m^2 s^{-1}	Fuller correlation [2]
Dynamic viscosity of H_2 at 300 K (η)	9×10^{-6} kg m^{-1} s^{-1}	[6]
Density of dry membrane ($\rho_{membrane}$)	1980 kg m^{-3}	[7] for Nafion® 117
Saturation concentration of H_2O in the membrane ($c_{H_2O,sat}$)	7521 mol m^{-3}	[1]

3. Temperature distribution inside the cell

3.1. Model properties

The temperature distribution inside the hydrogen–hydrogen cell used in this work was modeled in order to see when the non-isothermal effects should be included. Heat production by ohmic heating, activation losses, reaction entropy, and water phase change were taken into account. The produced heat was assumed to be transferred by conduction and convection. Both electrical and thermal contact resistances between different cell components were taken into account. GDB-electrode and GDB-flow field net boundaries were modeled as thin layers, and the conductivities of these layers were calculated from the values of the contact resistances. In order to be able to calculate the heat production rates and electro-osmotic water transport, the potentials of electron and proton conductors were also modeled. The average current density was $0.7\,\mathrm{A\,cm^{-2}}$, which was the maximum current density at which the solution converged. The details of the model are described in the following subchapters. Humidity conditions are the same as in measurement 17 in [1], i.e. dew-point temperatures of inlet gases are 33 °C.

3.2. Reaction kinetics and charge and mass transfer

Reaction kinetics is modeled with a linearized Butler–Volmer equation. The charge transfer rate at the anode is

$$j_{\mathrm{anode}} = \frac{j_0 z F \eta_{\mathrm{anode}}}{RT} = \frac{j_0 z F(\phi_{\mathrm{S}} - \phi_{\mathrm{M}})}{RT}, \tag{10}$$

and at the cathode

$$j_{\mathrm{cathode}} = \frac{j_0 z F \eta_{\mathrm{cathode}}}{RT} = \frac{j_0 z F(\phi_{\mathrm{M}} - \phi_{\mathrm{S}})}{RT}, \tag{11}$$

where j_0 is the exchange current density, z is the number of electrons participating in the reaction, F is the Faraday constant, η is the activation overpotential, R is the molar gas constant, T is the absolute temperature, and ϕ_{M} and ϕ_{S} are the potentials of proton and electron conductor, respectively.

Charge transfer in bulk components is modeled with the following equation

$$\vec{i} = -\sigma \nabla \phi, \tag{12}$$

where $\vec{i}$ is the current density and σ is the conductivity.

There are current sources in the electrodes and therefore the divergence of current density at the electrodes is equal to the charge transfer rate

$$\nabla \cdot (-\sigma \nabla \phi) = \pm j, \tag{13}$$

where the sign depends on the charge carrier and on the electrode. There are no current sources or sinks in any other component and therefore the divergence of current density is zero in other components.

Significant losses occur in a H_2–H_2 cell at the interfaces between cell components. Typically electrical contact losses are either neglected or modeled as stepwise discontinuities. Stepwise discontinuity makes it very challenging to take interfacial heating into account and it makes the numerical solution more time-consuming. Because of these reasons, interfaces were modeled as thin layers. The thickness of the layers was chosen to be 1 μm and their thermal and electrical conductivities were calculated from the contact resistance values. The contact resistance values were found from the literature only for graphite–gas diffusion backing contact and this value was used also for other interfaces.

The potential of electron conductor at the interface between the steel net and the graphite current collector was set to cell voltage at the anode side and to zero at the cathode side. Current carried by electrons through other boundaries was set to zero because of symmetry or insulation conditions. The protons cannot leave the MEA and therefore current carried by protons was set to zero at electrode-gas diffusion backing boundaries. The protonic current through other boundaries is also zero because of either symmetry or insulation condition.

Water and hydrogen transport was calculated with the same equations and boundary conditions as explained in Section 2, with the exception that water transport by electro-osmotic drag was also taken into account here. Water flux in the membrane was calculated with the following equation

$$\vec{J}_{\mathrm{H_2O}} = -D_{\mathrm{H_2O,membrane}} \nabla c_{\mathrm{H_2O,membrane}} - \frac{\lambda \sigma}{F} \nabla \phi_{\mathrm{M}}, \tag{14}$$

where λ is the electro-osmotic drag coefficient (number of water molecules transferred with one proton), and other symbols as described previously. Authors are not aware of published data for electro-osmotic drag coefficient of Gore membrane and therefore we used value 0.9, which was given for Nafion 117 stabilized with water vapor at 30 °C [3]. Because of the water transport by the electro-osmotic drag, the concentration of water vapor at cathode exceeds $2.2\,\mathrm{mol\,m^{-3}}$, which is the concentration of saturated water vapor at 35 °C. Oversaturated water vapor was assumed to be condensed evenly on the cathode electrode. This condensation was notified only as heat source term. Different transport properties of liquid water were not taken into account in this model and its effects on the effective porosity of cell components were also neglected.

3.3. Heat production and transfer

The heat transfer mechanisms included in this model are conduction and convection. The total heat flux is the sum of conductive and convective heat fluxes. The conductive heat flux was calculated with the Fourier law

$$\vec{q}_{\mathrm{cond}} = -k \nabla T, \tag{15}$$

where $\vec{q}_{\mathrm{cond}}$ is the conductive heat flux and k is the thermal conductivity.

Convective heat flux $\vec{q}_{\mathrm{conv}}$ was calculated with the following equation

$$\vec{q}_{\mathrm{conv}} = \vec{J}_i M_i C_i T, \tag{16}$$

where $\vec{J}_i$ is the molar flux, M_i is the molar mass, C_i is the heat capacity of component i (hydrogen or water). The heat capacity of water vapor was used for water.

There is ohmic heat production in every component and also in the boundary layers,

$$p_{\text{ohmic}} = \sigma(\nabla\phi)^2. \quad (17)$$

It must be noted that at the electrodes there is ohmic heat production caused by both electronic and protonic currents. Heat is produced at the electrodes also by activation losses

$$p_{\text{act}} = j\eta, \quad (18)$$

and due to reaction entropy production or consumption

$$p_{\text{S}} = -\frac{jT\Delta S}{zF}, \quad (19)$$

where ΔS is positive for endothermic anode reaction and negative for exothermic cathode reaction.

There is also heat production by condensation of oversaturated water vapor on the cathode. The condensation rate was calculated as a proportion of oversaturated water vapor from the total mass flow of water going out from the cathode side of the cell, i.e.

$$\dot{m}_{\text{condensation}} = \frac{c_{\text{H}_2\text{O}} - c_{\text{sat}}}{c_{\text{H}_2\text{O}}}\dot{m}_{\text{H}_2\text{O}} \quad (20)$$

where $c_{\text{H}_2\text{O}}$ is the concentration of water vapor, c_{sat} is the concentration of saturated water vapor at 35 °C, and $\dot{m}_{\text{H}_2\text{O}}$ is the total mass flow of water going out from the cathode side of the cell. The value of $\dot{m}_{\text{H}_2\text{O}}$ was calculated by integrating the water flux through the outlet boundary. Heat production by condensation was calculated with the following equation

$$p_{\text{condensation}} = \frac{\dot{m}_{\text{condensation}} L_{\text{condensation}}}{V_{\text{electrode}}}, \quad (21)$$

where $L_{\text{condensation}}$ is the specific latent heat of condensation, and $V_{\text{electrode}}$ is the volume of one electrode, i.e. the volume where condensation was assumed to take place.

The different heating mechanisms are sources of heat flux,

$$\nabla \cdot \vec{q} = \sum p. \quad (22)$$

The electrical and thermal parameter values and their references used in this modeling work are given in Table 2. The electrical and thermal conductivities of the boundary layers were calculated from the contact resistances so that the total through-plane resistance of boundary layer equals the contact resistance. The exchange current density for anode and cathode reactions was assumed to be the same and it was calculated from the values of charge transfer resistance, r_2, given in [1].

4. Results and discussion

4.1. Diffusion coefficient of water in the membrane

The only free parameter of the model was D_0, which was fitted into the measurement results obtained under one-phase conditions, i.e. measurements 1, 2, 5, 6, and 9 in [1]. The value of D_0 was varied with $1 \times 10^{-10}\,\text{m}^2\,\text{s}^{-1}$ steps until the difference between measured and modeled concentrations of water vapor reached its minimum. The resulting value for D_0 is $1.5 \pm 0.3 \times 10^{-9}\,\text{m}^2\,\text{s}^{-1}$. Diffusion coefficient of water in the membrane and its error limits as a function of membrane water concentration were calculated using Eq. (9) and are illustrated in Fig. 2. The diffusion coeffient illustrated in Fig. 2 is of same order of magnitude, but a little higher than the one reported in [3]. Differences can be explained with different membrane materials and various methods.

The modeled water concentration of measurement 2 in [1] is illustrated in Fig. 3 as an example. Measurement 2 was chosen, because it has the largest water flux and water concentration difference among the measurements conducted under one-phase conditions. The dew-point temperature of the gas entering the cell on side 1 was 33.4 °C, and the gas on side 2 was dry. Modeling result shows that in this case the water vapor

Table 2
Parameter values used to model temperature distribution

Parameter	Value	Reference
Electrical conductivity of gas diffusion backing (σ_{GDB})	$10000\,\Omega^{-1}\,\text{m}^{-1}$	[8]
Electrical conductivity of boundary layer (σ_{cont})	$1\,\Omega^{-1}\,\text{m}^{-1}$	Calculated from [8]
Electrical conductivity of electrode (σ_{S})	$570\,\Omega^{-1}\,\text{m}^{-1}$	Used in [5]
Electrical conductivity of steel net, σ_{net}	$1.3 \times 10^6\,\Omega^{-1}\,\text{m}^{-1}$	1/3 of pure AISI316
Ionic conductivity of membrane (σ_{membrane})	$0.00065\,\text{m}^2\,\text{mol}^{-1}\,\Omega^{-1} \cdot c_{\text{H}_2\text{O,membrane}}$	[1]
Volume fraction of proton conducting phase in electrode ($\varepsilon_{\text{membrane}}$)	0.24	Used in [9]
Ionic conductivity of electrode (σ_{M})	$\varepsilon_{\text{membrane}} \cdot \sigma_{\text{membrane}}$	
Thermal conductivity of steel net (k_{net})	$5\,\text{W}\,\text{m}^{-1}\,\text{K}^{-1}$	1/3 of pure AISI316
Thermal conductivity of gas diffusion backing (k_{GDB})	$7\,\text{W}\,\text{m}^{-1}\,\text{K}^{-1}$	[8]
Thermal conductivity of boundary layer (k_{cont})	$2 \times 10^{-3}\,\text{W}\,\text{m}^{-1}\,\text{K}^{-1}$	Calculated from [8]
Thermal conductivity of electrode (k_{ele})	$1.3\,\text{W}\,\text{m}^{-1}\,\text{K}^{-1}$	Used in [5]
Thermal conductivity of membrane (k_{membrane})	$0.455\,\text{W}\,\text{m}^{-1}\,\text{K}^{-1}$	Used in [5]
Exchange current density of anode and cathode reactions (j_0)	$1.7 \times 10^9\,\text{A}\,\text{m}^{-3}$	Calculated from [1]
Entropy change of anode and cathode reactions (ΔS)	$\pm 0.104\,\text{J}\,\text{mol}^{-1}\,\text{K}^{-1}$	[10]
Electro-osmotic drag coefficient (λ)	0.9	[3]
Heat capacity of hydrogen (C_{H_2})	$29.9\,\text{J}\,\text{mol}^{-1}\,\text{K}^{-1}$	[6]
Heat capacity of water vapor ($C_{\text{H}_2\text{O}}$)	$2040\,\text{J}\,\text{kg}^{-1}\,\text{K}^{-1}$	[6]
Specific latent heat of condensation ($L_{\text{condensation}}$)	$2.444 \times 10^6\,\text{J}\,\text{kg}^{-1}$	Calculated from [6]

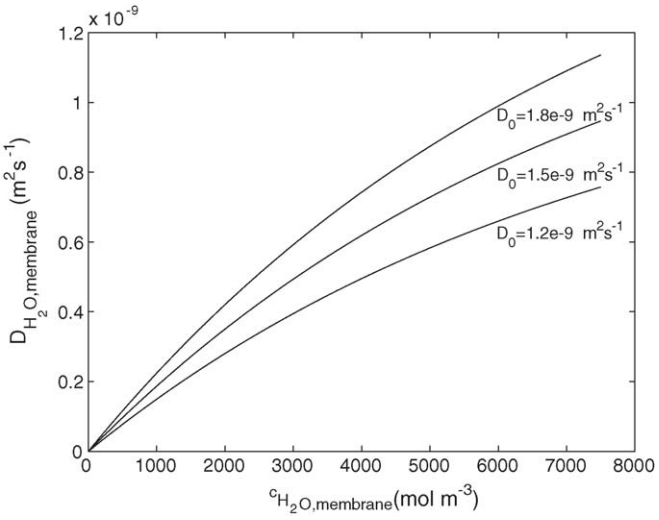

Fig. 2. Calculated $D_{H_2O,membrane}$ as a function of membrane water concentration.

concentration along the membrane surfaces varies from 1.3 to 1.6 mol m^{-3} on side 1 and from 0.3 to 0.7 mol m^{-3} on side 2. Differences are quite large and lead into significant concentration differences inside the membrane in the direction parallel to the membrane surfaces. The driving force for the diffusive water flux through the membrane is the concentration gradient, when also the diffusion coefficient is concentration dependent, the water flux through the membrane cannot be assumed uniform. This means that when the measurement technique explained in [1] is used to determine the membrane water transport properties, the modeling work is a very essential part of the result analysis.

It was assumed that the convective velocity of hydrogen–water vapor mixture is same as the convective velocity of hydrogen. The largest density changes occur in the conditions of measurement 2. It can be calculated from the modeling results

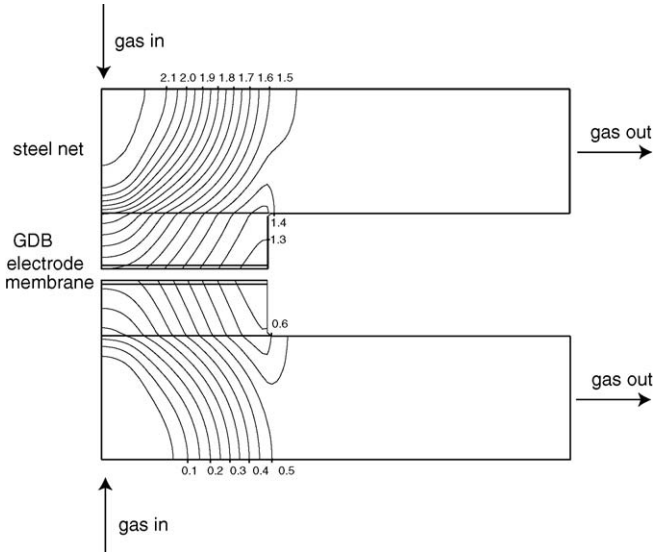

Fig. 3. Calculated water vapor concentration inside the cell. Numbers refer to the concentrations at contour lines (mol m^{-3}).

Table 3
Calculated and measured total membrane area-specific resistances

Measurement	Calculated area-specific resistance (10^{-6} Ω m^2)	Measured area-specific resistance (10^{-6} Ω m^2)
1	27.2	19.8
2	19.2	19.0
5	6.9	6.9
6	5.7	6.3

Measurement refers to the measurement conditions given in [1].

that the maximum changes in the density of the fluid are 10% and the assumption is valid.

4.2. Membrane conductivity

The conductivity of the membrane as a function of water concentration was calculated from the results of impedance measurements conducted with constant water concentration (measurements 15–17 in [1]). Eq. (13) and the modeling results for water concentration can be used to calculate the resistance of the membrane with a non-constant water concentration profile, i.e. for measurements 1, 2, 5, and 6 in [1], to cross-check the results. Calculation was done with COMSOL Multiphysics™ using the calculated water concentration profiles and adding a potential variable into the model. Potential profile was calculated using Eq. (13) for the membrane. Divergence of the current density is zero in the membrane. Potential difference over the membrane was fixed. Current through the side boundaries was fixed to zero.

Total current was calculated from the solution and the total resistance of the membrane was calculated using the Ohm law. Calculated total area-specific resistances are given in Table 3. The total area-specific resistances of the membrane achieved from the impedance measurements in [1] are also given in Table 3 and they are similar with calculated values. Taking into account the assumptions of the model and the accuracy of the measurements, this supports the consistency between the model and measurements.

4.3. Temperature distribution

The modeled temperature profile through the cell in dc-mode with 0.7 A cm^{-2} average current density is illustrated in Fig. 4. The temperature profile is plotted along the left boundary of the modeled geometry. 0.7 A cm^{-2} average current density was chosen, because it was the highest current density at which the solution converged. The maximum temperature inside the cell is approximately 1 °C larger than the temperature of the cell body, which implies that the cell can be treated as an isothermal system. The differences inside the bulk material are negligibly small, 0.1 °C at maximum. The temperature at the cathode side of the cell is slightly higher than the anode side, because of heat released in the condensation of water vapor at the cathode. The largest changes occur at the interfaces between the cell components, which indicate that the poor thermal conductivity of the boundary layers is the main reason for the temperature

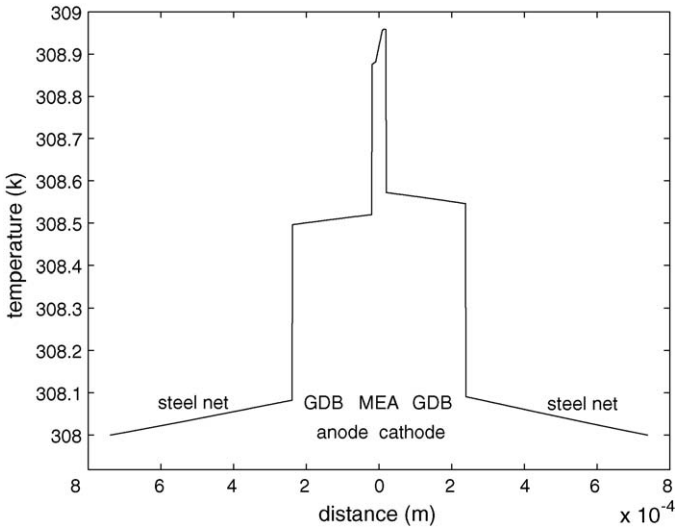

Fig. 4. Temperature profile through the cell at 0.7 A cm^{-2} average current density.

differences inside the cell. Therefore it is important to take interfacial losses into account in the modeling of the cell.

5. Summary and conclusions

Two-dimensional one-phase model for hydrogen and water transport in hydrogen-hydrogen cell was developed to determine the diffusion coefficient of water in the membrane as a function of humidity. Temperature distribution inside the cell was also modeled with a separate model to see if the cell can be treated isothermally. The modeled geometry was similar to the experimental cell used in [1] and the measurement results achieved in [1] were used for material parameters or boundary conditions.

A one-parameter exponential dependence for the diffusion coefficient of water on the humidity was developed and included into the transport model. This was the only free parameter of the model and it was varied until the modeling results matched the measurements. As a result, an estimate for the dependence of the diffusion coefficient of water on the humidity was found. The dependence can be used with Gore™ Primea® Series 58 MEA, which was used in the measurements. It must be noted that the value of the diffusion coefficient was calculated using the water uptake values of whole MEA. The given equation for the diffusion coefficient is valid only when the water uptake Eq. (8) is used.

The modeling results showed that there are significant concentration gradients along the membrane surfaces, which causes variation in water flux in transverse direction. Therefore modeling work is necessary if one wants to determine the diffusion coefficient of water with the presented method, i.e. by measuring the net water flux though the membrane. Without the modeling work one could get only cell-specific averaged value for the diffusion coefficient.

The resistance of the membrane was calculated using the modeled water concentration profiles and measured conductivity of the membrane. This was done to cross-check the modeling results, i.e. if the modeled water concentrations are realistic, calculated membrane resistances should be close to the measured values. Calculated and measured membrane resistances were in agreement.

The temperature distribution inside the hydrogen–hydrogen cell was modeled assuming that heat is transferred by conduction and convection and produced by resistive, activation, and reaction entropy losses, and also by heat released in the condensation of water vapor at the cathode. Temperature differences inside the cell were small even at 0.7 A cm^{-2} average current density and therefore the cell can be treated isothermally.

Acknowledgement

The financial support of the Academy of Finland (206132) is gratefully acknowledged.

Appendix A. Nomenclature

c	concentration (mol m^{-3})
C	heat capacity (J mol^{-1} K^{-1})
D	diffusion coefficient (m^2 s^{-1})
F	the Faraday constant (96,485 C mol^{-1})
$\vec{i}$	current density (A m^{-2})
j	charge transfer rate (A m^{-3})
j_0	exchange current density (A m^{-3})
$\vec{J}$	molar flux (mol m^{-2} s^{-1})
k	thermal conductivity (W m^{-1} K^{-1})
L	specific latent heat (J kg^{-1})
$\dot{m}$	total mass flow (kg s^{-1})
M	molar mass (kg mol^{-1})
p	pressure (Pa) or heat production (W m^{-3})
$\vec{q}$	heat flux (W m^{-2})
r	distance (m) or area-specific resistance (Ω m^2)
R	the molar gas constant (8.314 J mol^{-1} K^{-1})
S	entropy (J mol^{-1} K^{-1})
T	temperature (K or °C)
$\vec{v}$	velocity (m s^{-1})
V	volume (m^3)
WU	water uptake
z	number of electrons

Greek letters

Δ	change
ε	porosity
η	dynamic viscosity (kg m^{-1} s^{-1}) or activation overpotential (V)
κ	hydraulic permeability (m^2)
λ	electro-osmotic drag coefficient
ρ	density (kg m^{-3})
σ	conductivity (Ω^{-1} m^{-1})
ϕ	potential (V)

Superscripts and subscripts

calc	calculated
cond	conductive

conv	convective
H_2O,membrane	water in the membrane
meas	measured
M	proton conductor
sat	saturation
S	electron conductor

References

[1] O. Himanen, T. Hottinen, M. Mikkola, V. Saarinen, Electrochim. Acta, 2006.
[2] E. Fuller, P. Schettler, J. Giddings, J. Ind. Eng. Chem. 58 (1966) 18.
[3] T. Zawodzinski, C. Derouin, S. Radzinski, R. Sherman, V. Smith, T. Springer, S. Gottesfeld, J. Electrochem. Soc. 140 (1993) 1041.
[4] M. Williams, E. Begg, L. Bonville, H. Kunz, J. Fenton, J. Electrochem. Soc. 151 (2004) A1173.
[5] P. Nguyen, T. Berning, N. Djijali, J. Power Sources 130 (2004) 149.
[6] CRC Handbook of Chemistry and Physics, 78th ed., CRC Press, ISBN: 0-8493-0478-4.
[7] http://www.dupont.com/fuelcells/pdf/nae101.pdf, cited 21.10.2005.
[8] J. Ihonen, M. Mikkola, G. Lindbergh, J. Electrochem. Soc. 151 (2004) A1152.
[9] N. Siegel, M. Ellis, D. Nelson, M. von Spakovsky, J. Power Sources 128 (2004) 173.
[10] M. Lampinen, M. Fomino, J. Electrochem. Soc. 140 (1993) 3537.